

Application of Ultrasound for Start-Up of Evaporative Batch Crystallization of Ammonium Sulfate in a 75-L Crystallizer

Richard Lakerveld, Nelleke G. Verzijden, Herman Kramer, and Peter Jansens
Dept. of Process and Energy, Delft University of Technology, Delft, The Netherlands

Johan Grievink
Dept. of DelftChemTech, Delft University of Technology, Delft, The Netherlands

DOI 10.1002/aic.12553

Published online March 22, 2011 in Wiley Online Library (wileyonlinelibrary.com).

A positive effect of ultrasound on crystallization has been shown for many applications especially on small scale. Predictable scale-up of sonocrystallization is a challenge due to the inherent dependency of ultrasound on scale. The presented research discusses the experimental application of ultrasound to induce nucleation at low supersaturation for start-up of evaporative batch-wise crystallization of ammonium sulfate in a 75-L draft tube (DT) crystallizer. A comparison is made with a conventional start-up procedure using primary nucleation or seeding. Ultrasound is applied in two geometrically different vessels of 1.2-L connected to a 75-L DT crystallizer. Application of ultrasound for start-up of a 75-L DT crystallizer shows that an optimum amount of ground seeds is better capable to suppress nucleation. A challenge for future research is to improve the efficiency of ultrasound to produce a large number of nuclei for start-up of batch crystallization at larger scale. © 2011 American Institute of Chemical Engineers AIChE J, 57: 3367–3377, 2011

Keywords: crystallization, ultrasound, seeding, sonocrystallization, nucleation

Introduction

Batch crystallization is a widely applied separation and product formation technology in chemical industry. The future impact of crystallization is expected to increase as new high-added value products are often in crystalline form and need to comply with increasingly stringent product quality requirements. The start-up of batch crystallization is of key importance to minimize batch to batch variations and to obtain a desired final product quality. In the initial phase of a batch, supersaturation can be increased to such a high level that primary nucleation is provoked. Fast growth of the crystals due to the high supersaturation increases the impurity

content of the crystals and it affects the crystal shape. This high supersaturation can also cause crystal deposition on the interior of the processing compartment. Furthermore, the initial number of crystals formed by primary nucleation is difficult to predict and control. Seeding can be considered as an alternative for primary nucleation. It offers more flexibility for design as seed properties can be optimized for a given design objective. However, the application of seeding is not straightforward and requires careful optimization for each application.¹ Furthermore, additional equipment is required to prepare the seed crystals in slurry and additional protocols related to hygiene are required, which is especially important for food and pharmaceutical industry.

Ultrasound can potentially be used to improve the control over the generation of the initial crystals in batch crystallization. The capability of ultrasound to discharge metastable systems such as supersaturated solutions has already been

Correspondence concerning this article should be addressed to R. Lakerveld at rlakerv@mit.edu.

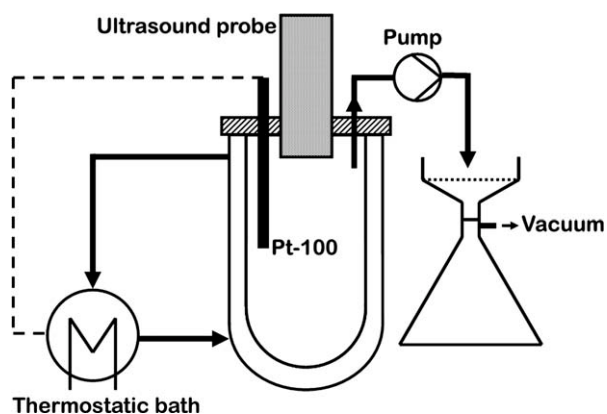


Figure 1. Experimental setup for quantification of the crystal production by insonation.

Two vessels with different aspect ratio were tested. One of the two vessels will be used for start-up of a 75-L DT crystallizer.

reported in the late 20s.² For many crystallizing components in different solvents, it has been shown that ultrasound can reduce induction time and decrease the mean crystal size compared to batch crystallization using conventional primary nucleation.^{3–15} It should be noted that the application of ultrasound does not always enhance nucleation and an inhibition of nucleation also has been reported for certain operating conditions.^{10,11,15} Furthermore, experimental studies showed that ultrasound can be effective in preventing agglomeration.^{3,8,16,17} For some systems, it has been shown that ultrasound can induce attrition of existing crystals^{14,18} whereas for other systems no attrition could be detected.¹⁵ On a case to case basis, several researchers demonstrated improved crystallization enabled by ultrasound for a broad range of systems.^{17,19–25} The mechanism explaining the influence of ultrasound on crystallization phenomena has been a topic of debate for many decades. Ultrasonic waves can create cavities in the solution, enhance mixing and transfer heat, which all can be potential sources of the experimentally observed effects.

The translation of ultrasound from experiments on a laboratory scale to an industrial process is not a trivial task. This is mainly caused by a lack of fundamental understanding of key physical phenomena and by the inherent dependency of the scale of operation on the effectiveness of ultrasound. A typical distance over which an intensive field by an ultrasonic probe can be transferred is around 2–5 cm.²¹ Therefore, in case of a small lab-scale setup it is possible to insonate most of the working volume and therefore observe a significant effect of ultrasound on crystallization for the studied cases. However, on a larger scale, it is difficult to insonate a large part of the working volume, which requires different methods and thus a different product quality compared to the lab-scale experiments can be expected. Systematic and quantitative comparisons of the use of ultrasound with other methods for start-up of batch crystallization are mainly available for laboratory scale only.

The aim of this article is to compare the performance of batch crystallization by using ultrasound and conventional methods (primary nucleation and seeding) for start-up on a

pilot plant scale. The performance of the batches will be judged based on batch to batch reproducibility of the crystal size distribution (CSD) and the obtained final product quality in terms of CSD, which preferably has a large median size and narrow distribution width for the studied case. A 75-L draft tube (DT) crystallizer operated in evaporative fed-batch mode for crystallization of ammonium sulfate from aqueous solution is studied. An ultrasonic probe is used in a smaller vessel, which is connected to the 75-L DT crystallizer, to generate the initial crystals with ultrasound. The article is divided into two main parts. In the first part, the generation of the initial population with ultrasound will be quantified by varying insonation time and power input in a small vessel. Two different geometries for the insonated volume will be tested. In the second part, an initial population generated with ultrasound in the small vessel will be used for start-up of the 75-L DT crystallizer and compared to results from literature¹ involving start-up with conventional primary nucleation and different seeding methods.

Quantification of Nuclei Production with Ultrasound

Experimental setup

A schematic drawing of the experimental setup that was used to quantify the production of nuclei with ultrasound is given in Figure 1. Two different vessel geometries (referred to as vessels A and B) were tested for insonation with equal volume but different aspect ratio (Figure 2). They both were 1.2-L jacketed vessels made out of glass with a concave bottom. The concave bottom reflected the waves back into the vessel, which provided mixing (similar as Abbas et al.²⁵). A magnetic stirrer was used to stir the vessels when ultrasound was not applied. The vessels were closed to prevent evaporation of solvent. At the top of the vessel, an ultrasonic probe connected to a power generator (UIP 250, Hielscher Ultrasonics GmbH) was placed with the tip (\varnothing 4.0 cm) just

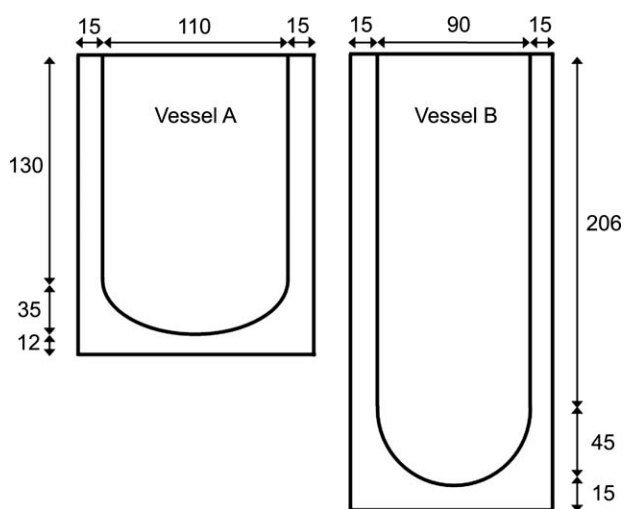


Figure 2. Dimensions (mm) of the vessels in which ultrasound was applied.

Vessel A was connected to the 75-L DT crystallizer to generate the initial crystal population with ultrasound for start-up of the batch.

immersed into the liquid. The maximum power input of the probe was 250 W with a fixed frequency of 24 kHz. Ultrasound was applied with pulses of 0.5 s delivered at 1 Hz. The power that was actually transferred to the liquid could be varied between 0 and 88 W, which was calibrated by measuring the temperature increase in vessel A in case of adiabatic operation. The dependency between power output of the generator and actual power that was transferred into the liquid was linear. The temperature inside the vessel was controlled by an external Pt-100 connected to a thermostatic bath (Ecoline Staredition RE310, Lauda). Both vessels could be connected to the 75-L DT crystallizer, which allowed for rapid introduction of the produced crystals into the bulk of the vessel at start-up.

First, both vessels were tested separately from the 75-L DT crystallizer to quantify the generation of crystals as function of power input and insonation time. A saturated ammonium sulfate water solution was prepared in a stirred 10-L jacketed vessel by adding an excess of ammonium sulfate (DSM, technical grade) to demineralized water at least 1 day before the experiment. An external Pt-100 was connected to a thermostatic bath (Ecoline Staredition E300, Lauda) to control the temperature inside the vessel. The solution was pumped to vessel A or B by using a filter to assure only liquid was transferred and ultrasound was applied pulse-wise at maximum power for 1 min to de-aerate the solution. The temperature of the liquid was maintained at 5°C above saturation for at least 1 h to assure a crystal-free solution after which it was cooled with $0.25^{\circ}\text{C min}^{-1}$ to a temperature within the metastable zone. At this temperature, ultrasound was applied to induce nucleation. A small temperature rise in the bulk resulted from insonation, which did not exceed the metastable zone. For these experiments, no additional supersaturation was generated during insonation and therefore only the initial supersaturation was fixed. After insonation, the solution was cooled 2 more degrees with a rate of $0.2^{\circ}\text{C min}^{-1}$ to the final temperature of the experiment to grow the crystals, which improved the accuracy of sampling and CSD measurements. It was assumed that during this growth phase the number of crystals remained constant. A number of experiments were done in duplo to validate this assumption and no significant change in number of crystals was measured as a result of a different final temperature. At the end of each experiment, the remaining solution and the produced crystals were pumped out of the vessel with a peristaltic pump. The solids were separated from the liquid by using vacuum filtration. Ethanol was used to wash the crystals after which they were dried in an oven at 50°C. The crystal yield was weighed and the CSD was measured with a laser diffraction instrument (S3500, Microtrac) from which the number of produced crystals was calculated.

Experimental program

There are various degrees of freedom that potentially manipulate the amount of produced crystals by using ultrasound such as

1. power,
2. insonated volume,
3. ultrasound frequency,
4. frequency of applied pulsing,

5. time horizon over which the pulsing is applied,
6. transducer type,
7. traveling distance of ultrasonic waves before reflection,
8. temperature, and
9. supersaturation.

A selection of manipulated variables has to be made since the combination of available manipulated variables is too exhaustive. Therefore, only near optimal conditions for insonation can be found. Furthermore, the objective of this work is not fully optimize batch crystallization of $(\text{NH}_4)_2\text{SO}_4$ on small scale, but rather to compare the use of ultrasound for start-up of batch crystallization on pilot plant scale with alternative methods such as seeding and conventional primary nucleation. The traveling distance of the ultrasonic waves was believed to have a significant impact on the nucleation due to the exponential attenuation of ultrasonic intensity with distance.²⁶ It was decided to manipulate the traveling distance and keep volume constant by employing two vessels with different aspect ratio. The transducer type and ultrasound frequency were fixed by the used equipment. The final temperature after insonation was constrained by standard operating conditions of the 75-L DT crystallizer and pulsation conditions of the ultrasound were not changed. The latter could potentially be changed if the temperature rise in the bulk was too high. The supersaturation at which ultrasound is applied can have a significant effect on the nucleation behaviour.²⁷ Nevertheless, supersaturation was kept low, because an interesting aspect of ultrasound is that it can be applied in situ for which supersaturation should be low to prevent uncontrolled nucleation. The time and power input of insonation were varied. The descriptions of the conducted experiments are given in Table 1. A reference experiment was done in which the solution simply was cooled until primary nucleation occurred. Note that the nucleation in the reference experiments normally occurred at much higher supersaturation due to the absence of cavities induced by ultrasound, which was visually observed.

For the experiments described in Table 1, no additional supersaturation was created during insonation. However, it was expected that the production of nuclei decreased once supersaturation became depleted (similar to Kordylla et al.⁹). In principle, the production of the crystals with ultrasound could be further optimized for example by applying ultrasound during a cooling ramp, which increased the time at which ultrasound could be applied to a sufficiently supersaturated solution. Therefore, an additional set of experiments was done in which a solution saturated at 65°C was cooled to 50°C with a cooling curve, which aimed to maintain supersaturation during insonation. The shape of such a cooling curve can be derived from component balances and the population balance simplified to moment balances, which under assumption of size-independent growth and constant values for supersaturation, nucleation rate, volume, liquid density, and solid density are given respectively as

$$\frac{d[V \cdot \varepsilon \cdot w \cdot \rho_L + V \cdot (1 - \varepsilon) \cdot \rho_S]}{dt} = 0 \quad \forall t \in (t_0, t_f],$$

$$\varepsilon(t_0) = 1, \quad w(t_0) = w_0 \quad (1)$$

Table 1. Experimental Conditions for Quantifying the Crystal Production by Ultrasound (Figure 1)

ID	Number of Experiments	T_{US} (°C)	Power (W L ⁻¹)	Insonation Time (min)	Vessel
ref	2	—	—	0	A
A1	2	54	42	2	A
A2	4	54	52	2	A
A3	2	54	62	2	A
A4	2	54	72	2	A
A5	2	54	52	6	A
A6	2	54	52	12	A
A7	2	54	52	18	A
A8	1	54	52	60	A
B1	3	52	52	25	B
B2	1	52	52	6	B
B3	1	54	52	18	B
B4	1	54	80*	18	B

No additional supersaturation was generated with $\sigma_{\text{initial}} = 0.20\%$ for all cases.

*Working volume was decreased to 0.8 L.

where V represents the working volume, ε the volumetric liquid fraction, w the weight fraction of solute, and ρ the density.

$$\frac{dm_0}{dt} = B \quad \forall t \in (t_0, t_f], \quad m_0(t_0) = 0 \quad (2)$$

$$\frac{dm_i}{dt} = i \cdot m_{i-1} G \quad \forall i = 1, 2, 3, \quad t \in (t_0, t_f], \quad m_i(t_0) = 0 \quad (3)$$

where m_i is the i th moment of the CSD, B the nucleation rate, and G the growth rate. The connection between the mass balance and moment balances is provided by

$$\varepsilon = 1 - k_V m_3 \quad (4)$$

where k_V is the volumetric shape factor. The relative supersaturation σ is defined as

$$\sigma_c = \frac{w - w^*}{w^*} \quad (5)$$

with for an ammonium sulfate water system²⁸

$$w^* = 0.41179 + 9.121 \cdot 10^{-4} \cdot (T - 273) \quad T \in [267, 353] \quad (6)$$

Integration of Eq. 1 using the specified initial conditions gives:

$$w(t) = \frac{\rho_L \cdot w_0 - \rho_S \cdot [1 - \varepsilon(t)]}{\rho_L \cdot \varepsilon(t)} \quad (7)$$

The temperature profile that has to be applied for constant supersaturation follows from Eqs. 5–7

$$T(t) = \frac{\rho_L [w_0 - 0.41179 \cdot \varepsilon(t) \cdot (1 + \sigma_c)] - \rho_S \cdot [1 - \varepsilon(t)]}{9.121 \cdot 10^{-4} \cdot \rho_L \cdot \varepsilon(t) \cdot (1 + \sigma_c)} \quad (8)$$

With (by applying analytical integration of Eq. 2–4)

$$\varepsilon(t) = 1 - \frac{1}{4} \cdot k_V \cdot t^4 \cdot G^3 \cdot B \quad (9)$$

The nucleation rate B was assumed to be constant as supersaturation and insonation conditions were constant. An estimated value of $4 \times 10^8 \text{ m}^{-3} \text{ s}^{-1}$ was chosen based on the results of previous experiments (Figure 3). From Eqs. 8 and 9, it can be seen that the cooling profile was strongly dependent on the growth rate, which was difficult to predict accurately. Therefore, the experiments were done for different growth rates spanning almost one order of magnitude, which effectively changed the steepness of the cooling profile. In this way also, other model uncertainties were implicitly taken into account as the model was used to determine the optimal cooling profile. In addition, the constant supersaturation level σ_c was varied, which varied the starting point of the cooling curve and also influenced the steepness of the cooling curve according to Eq. 8. A solution saturated at 65°C was prepared and transferred to vessel A. The solution was kept at 75°C for at least 30 min to dissolve all crystals after which it was cooled with $0.4^\circ\text{C min}^{-1}$ to a temperature corresponding to the chosen supersaturation σ_c . Insonation was started at that point and the solution was cooled according to Eq. 8. A maximum temperature gradient of $0.5^\circ\text{C min}^{-1}$ was imposed to prevent a large temperature difference between the jacket and the bulk. At this point, supersaturation was still generated but at a lower rate than necessary to maintain supersaturation as predicted by the model. The effect of ultrasound during this period was uncertain as potentially new nuclei could be generated, but nuclei could also dissolve due to local hot spots caused by the ultrasonic field and a low supersaturation in the bulk. Therefore, the decision to insonate the solution during the period constrained by the maximum temperature gradient was also taken as a degree of freedom for the experiments. An overview of the experimental conditions is given in Table 2.

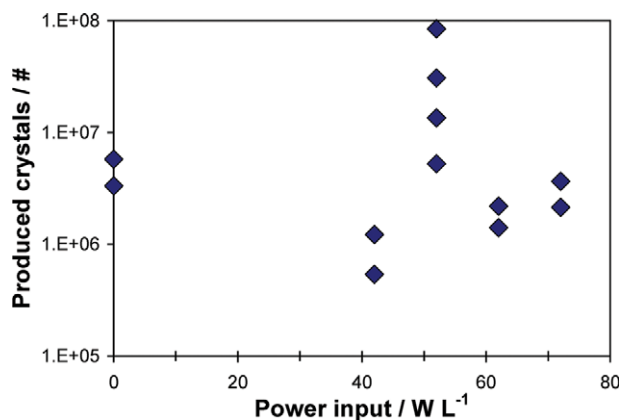


Figure 3. Number of produced crystals for different ultrasonic power input at an insonation time of 2 min in vessel A (experiments ref, A1–A4 from Table 1).

[Color figure can be viewed in the online issue, which is available at www.interscience.wiley.com.]

Table 2. Experimental Conditions for Quantifying the Crystal Production by Ultrasound (Figure 1) with Cooling Ramp

ID	Number of Experiments	σ_c (%)	G (m s ⁻¹)	Ultrasound if Temperature Gradient Constrained?	Insonation Time (min)
S1	2	0.10	1×10^{-7}	yes	34
S2*	2	0.10	1×10^{-7}	yes	34
S3†	2	0.10	1×10^{-7}	yes†	10
S4	1	0.10	1×10^{-7}	no	6
S5	2	0.05	7×10^{-8}	no	10
S6	1	0.10	2×10^{-8}	no	24
S7	2	0.20	4×10^{-8}	no	14
S8	1	0.30	6×10^{-8}	no	11
S9‡	2	NA	NA	NA	0

Additional supersaturation was generated by applying a cooling ramp.

*Magnetic stirrer used during insonation.

†No constraint on maximum temperature gradient imposed, but determined by equipment.

‡Reference experiment, cooling profile as for experiment S6.

Experimental results quantification crystal production with ultrasound

In the experiments with vessel A, tiny crystals in the order of magnitude of 10 μm were typically seen 1 min after the start of insonation. To use ultrasound in an effective start-up strategy for an industrial crystallizer, the number of crystals produced by ultrasound should be quantified first. The number of crystals that was produced in vessel A was dependent on the power input of the ultrasound probe (Figure 3). A maximum was found at an intermediate power input of 52 W L^{-1} . A certain minimum power input was necessary to exceed the threshold for formation of cavities for which Ruecroft et al.²¹ gave a typical value of 35 W L^{-1} . Above this threshold cavities were created, which explains the increased number of produced crystals at 52 W L^{-1} for our case. Upon further increasing the power input, the number of produced crystals decreased, which is more difficult to explain. The increase in the number of cavities with increasing power input is normally less than proportional, which might be caused by a shielding effect of cavities close to the tip of the probe.²⁹ In addition, more heat is transferred to the solution at higher power input, which might result in dissolution of nuclei. The bulk temperature typically showed a

small peak at the start of insonation and did not exceed the solubility line during the experiment. However, local hot spots might be present in the vessel, which can cause dissolution. The reproducibility of the experiments was satisfactory at least in terms of general trend. The results around the maximum show the most significant variation.

In subsequent experiments, the insonation time was increased at constant power input. The results in terms of number of produced crystals are given in Figure 4. A maximum in crystal nucleation was found around 6 min of insonation time. Apparently most of the supersaturation was consumed after this time, which prevented the formation of new crystals. Small temperature fluctuations due to the heat input of the probe might even reduce the number of particles at these conditions, which also explains the affected reproducibility of the experiments at longer insonation time. One experiment was done with a long insonation time of 60 min to evaluate the influence of attrition caused by collapsing bubbles (see, for example, Amara et al.¹⁴ and Kim et al.¹⁸). The number of produced crystals after 60 min was small from which it was concluded that attrition induced by ultrasound was not an important mechanism for our system and crystal population. The same graph also contains the results obtained by varying insonation time for vessel B, which has a larger aspect ratio. In this vessel, the insonation time did not affect the number of produced crystals for any of the tested conditions. Furthermore, the number of produced crystals was lower compared to the results from vessel A. Figure 5 shows scanning electron microscope pictures of produced crystals near the maximum in number of produced crystals from vessel A (experiment A2) and of crystals produced in vessel B (experiment B2). Besides the difference in mean size, a difference in crystal morphology could be observed. The edges and corners of crystals produced in vessel B grew faster compared to the facets, which was the result of diffusion limited growth at a high supersaturation. Apparently only a small amount of nuclei was produced, which subsequently grew out at high supersaturation after which a second burst of nucleation might have occurred. The multimodal size distribution that can be observed in the SEM picture was confirmed by measurement of the CSD (Figure 6). In case ultrasound was effective (left picture of Figure 5), this morphology was not observed indicating lower supersaturation during the growth phase of the experiment due to a larger amount of generated nuclei. The measured CSD showed a single peak at smaller size classes with a tail on

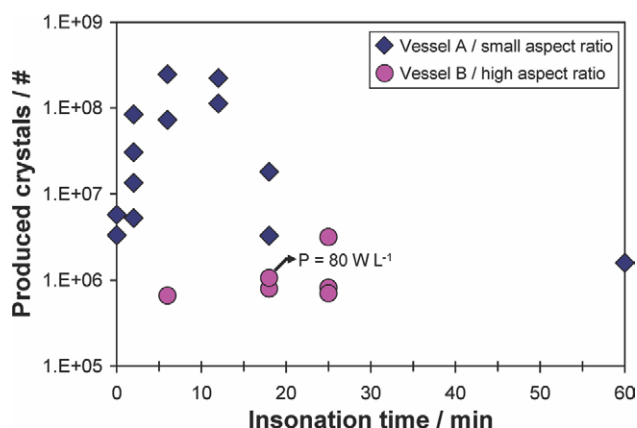


Figure 4. Number of produced crystals for different insonation time at a power input of 52 W L^{-1} in vessels A (◆, in blue) and B (●, in pink).

One experiment (SV6) was done at a higher power input of 80 W L^{-1} as indicated by the arrow (experiments A5–B4 from Table 1). [Color figure can be viewed in the online issue, which is available at wileyonlinelibrary.com.]

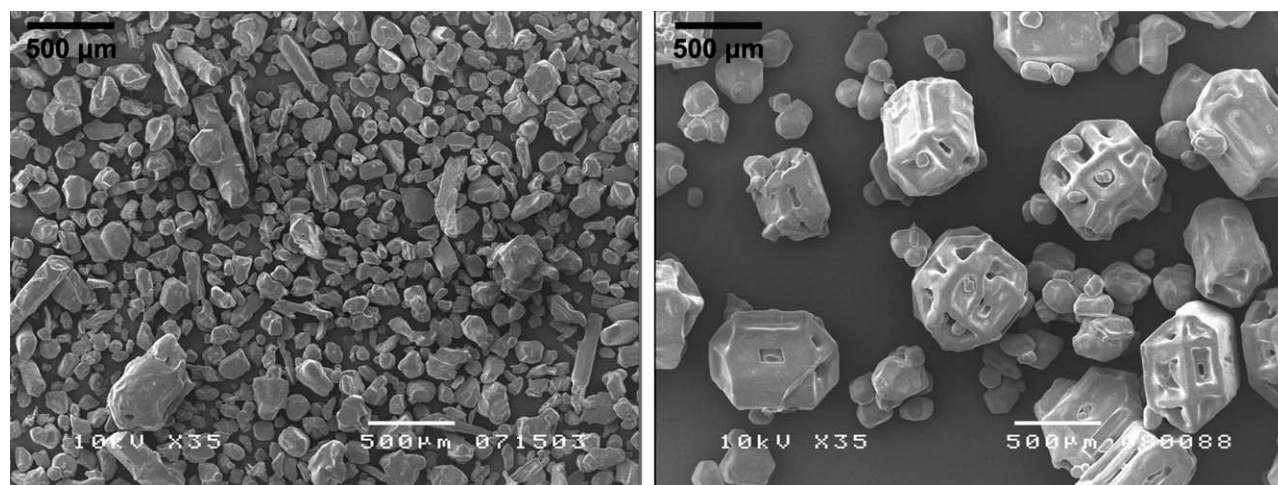


Figure 5. SEM pictures of crystals produced in vessel A with effective ultrasound (left, experiment A2) and from vessel B with ineffective ultrasound (right, experiment B2).

the larger size classes (Figure 6), which might be caused by agglomeration or nucleation during filtration of the sample as some needles could be seen on the SEM pictures.

The reason why the vessel with a larger aspect ratio and equal volume was less effective for generating nuclei with ultrasound is not fully understood. The height of the liquid in vessel B was around 20 cm, which is higher than a typical distance over which an intense field of cavitations can be transmitted. This is typically 2–5 cm.²¹ In vessel A with a smaller aspect ratio, the field might propagate more in radial direction creating more cavities. Another explanation might be related to mixing. In case of vessel B, the ultrasonic waves have to travel further before being reflected by the concave bottom. Temperature gradients might result as a consequence of decreased mixing, which can potentially dissolve the produced nuclei. The presented results demonstrate the importance of designing an effective geometry in which ultrasound is applied.

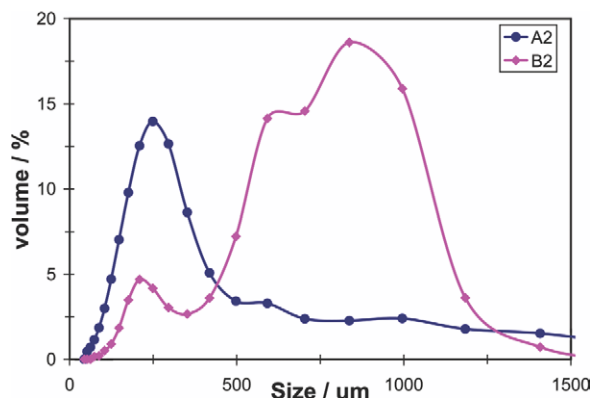


Figure 6. CSD of crystals produced in vessel A with effective ultrasound (experiment A2) and from vessel B with ineffective ultrasound (experiment B2).

[Color figure can be viewed in the online issue, which is available at www.interscience.wiley.com.]

In subsequent experiments, a cooling profile was applied in vessel A to maintain supersaturation for a longer period of time (Table 2). The numbers of produced crystals for these experiments are presented in Figure 7. It can be seen that for those experiments no significant effect of ultrasound on the number of produced crystals was observed. No clear trends were visible and there was no significant difference compared to experiments in which ultrasound was not applied. The supersaturation was not measured during the experiments, but predicted off-line with a model. The model contained assumptions such as constant nucleation rate and size independent growth. Furthermore, the obtained cooling profile was strongly dependant on the growth rate, which was difficult to estimate. This was taken into account by varying the growth rate, which effectively manipulated the cooling profile between experiments. Nevertheless, the real supersaturation might have deviated significantly from the predicted supersaturation. A small cooling rate results in depletion of supersaturation, which potentially results in dissolution of nuclei. A fast cooling rate might provoke primary nucleation after which supersaturation will be depleted rapidly. The strategy with a cooling ramp during insonation was not applied for start-up of the 75-L DT crystallizer since no clear effect of ultrasound was observed. In principle, the number of crystals produced with ultrasound has to be maximized to consume most supersaturation in the 75-L DT crystallizer. Inspection of the full CSD of the crystals with the larger numbers shows that especially the small size classes are filled and the mean size is not significantly smaller. These crystals in the small size classes are more sensitive for dissolution, which might result in (partial) dissolution after introduction into the crystallizer creating ill defined initial conditions. Dissolution was shown to be especially important for our experimental setup.¹ Therefore, for our application, it was chosen to use a power input of 52 W L⁻¹ and an insonation time of 18 min corresponding to experiment A7 for the start-up of the 75-L DT crystallizer as described in the next sections. These conditions for insonation represent a trade-off between a large number of crystals and the absence of very fine crystals.

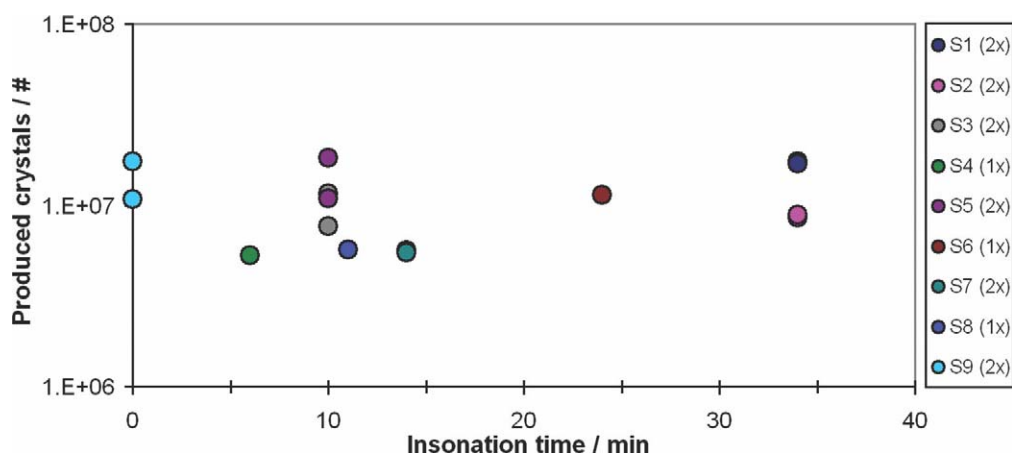


Figure 7. Number of produced crystals for different insonation times at a power input of 52 W L^{-1} applied during cooling (Table 2).

Note that the measurements of duplo experiments S1, S2, and S7 are very close and are difficult to distinguish. [Color figure can be viewed in the online issue, which is available at wileyonlinelibrary.com.]

Application of Ultrasound for Start-up of 75-L DT Crystallizer

Experimental 75-L DT crystallizer

The crystals produced with ultrasound were introduced in a 75-L DT crystallizer operated in evaporative fed-batch mode. Two identical experiments were done. Vessel A was connected to the pilot-plant crystallizer (Figure 8). Note that although a separate vessel was used, the step to in situ operation of ultrasound is very small as ultrasound could be

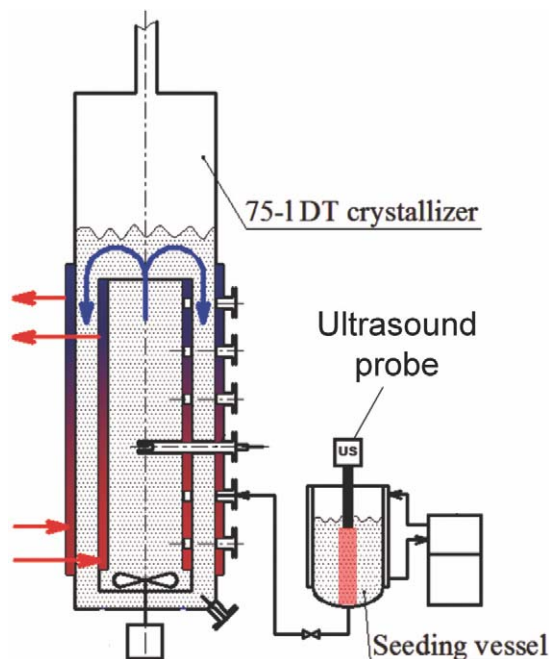


Figure 8. 75-L DT crystallizer connected with vessel A for production of initial crystal population with ultrasound.

For the seeded batch experiments vessel A was replaced with a stirred 5-L jacketed seeding vessel. [Color figure can be viewed in the online issue, which is available at wileyonlinelibrary.com.]

applied inside the crystallizer at the same conditions in a specifically designed compartment for ultrasound. This would require redesign of the crystallizer, which was simply avoided by the use of an external vessel. A solution saturated at 53°C was placed in the vessel and kept at 58°C for at least 1 h to assure that the solution was free of crystals after which it was cooled with $0.25^\circ\text{C min}^{-1}$ to 52°C . At this temperature ultrasound was applied for 18 min at 52 W L^{-1} after which it was cooled further to 50°C with $0.2^\circ\text{C min}^{-1}$ to allow the crystals to grow further and consume all supersaturation. Note that the same temperature difference was used as for the experiments described in the previous section, but temperatures were shifted 2°C lower to match the standard conditions in the 75-L DT crystallizer. The crystals were directly injected into the crystallizer as soon as the temperature reached 50°C and supersaturation in the 75-L DT crystallizer was within the metastable zone below the lower primary nucleation threshold of $\sigma = 0.0121$. The supersaturation was measured prior to the seeding point with a LiquiSonic probe (LiquiSonic® 20 with 24-24 TriClamp probe, SensoTech). The CSD was measured on-line during the batch every 2 min with a laser diffraction instrument (HELOS Vario, Sympatec). The heat input had a constant value of 120 kW m^{-3} , which resulted in a final theoretical yield of each batch of 33 kg. The operating temperature was fixed at 50°C by controlling the pressure ($\sim 80 \text{ mbar}$) and the stirrer speed was fixed at 450 rpm.

The performance of start-up with crystals produced with ultrasound was compared to the performance of seeds prepared in different ways. For those seeded experiments a 5-L jacketed vessel was connected to the crystallizer in which the seeds were prepared. A summary of the experiments is given in Table 3. A seeding procedure has been developed with ground seeds of which two experiments are taken with an optimal amount of seeds.¹ Furthermore, seeds were produced by adding 1 ml of antisolvent (ethanol) to a saturated solution of 55°C in the seeding vessel. The solution was cooled 5°C prior to seeding to increase the size of the seeds. It was observed with an in-line PVM probe (PIA524, MTS) that agglomeration took place in the seeding vessel, which

Table 3. Experimental Conditions Experiments in 75-L DT Fed-Batch Crystallizer for Evaporative Crystallization of Ammonium Sulfate from Water

ID	Seed Production Method	Seed Median Size (μm)	Start-up Conditions		
			Seed Mass (g)	Crystal Content Seed Slurry (vol %)	Initial Supersaturation 75-L σ_0
DTc13	Unseeded	—	—	—	Not measured
DTc15	Unseeded	—	—	—	0.02837
DTc17	Unseeded	—	—	—	Not measured
DTc18	Unseeded	—	—	—	0.02205
DTc19	Unseeded	—	—	—	0.01743
DTc31	Ground seeds	230	600	14.50	0.01286
DTc37	Ground seeds	230	600	14.50	0.01305
DTc59	Antisolvent	$\sim 170^*$	52	0.59	0.00627
DTc60	Antisolvent	$\sim 170^*$	52	0.59	0.00575
DTc61	Antisolvent	$\sim 170^*$	52	0.59	0.00572
DTc71	Ultrasound	240	7.6	0.36	0.00577
DTc72	Ultrasound	240	7.6	0.36	0.00478

*Agglomeration observed.

decreased the specific surface area of these seeds significantly. It should be noted that no efforts were made to optimize the seeding procedure with antisolvent. In the context of this work it is used as an example of the growth behavior in case the initial crystal population clearly has a small surface area. Finally, a number of unseeded experiments were used as reference.¹

Experimental results 75-L DT crystallizer with different start-up methods

The development of the CSD in terms of median size and distribution width for the experiments in which the initial crystal population was generated with ultrasound are given in Figure 9. It can be seen that the reproducibility between the two batches was good, which indicated that the initial distribution for both experiments was the same. The data provided by the LiquiSonic probe showed that seeding for experiment DTc71 and DTc72 occurred at a relative supersaturation of 0.0058 and 0.0048, respectively, which was well below the primary nucleation threshold.

The performance of the seeds was compared with unseeded experiments and experiments with two different types of seeds (Table 3). Figures 10–12 show the develop-

ment of median size and distribution width for those experiments. The use of ground seeds resulted in the smallest distribution width and slightly higher median size compared to the seeds produced with ultrasound. It was found in the previous section that the produced seed crystals with ultrasound were quite large and therefore had less surface area compared to the ground seeds which had a much higher seed mass. It can be seen that the ground seeds are more effective in suppressing secondary nucleation as the distribution width dropped more rapidly in the beginning (Figure 11). The initial growth of the seeds produced with antisolvent was much faster, which indicated an even higher supersaturation caused by a lack of available surface area for supersaturation consumption. The steep increase in median size was followed by a sudden decrease in growth and a changing trend in distribution width indicating a nucleation burst. It is typical growth behavior that can be expected when the initial population does not have a sufficient surface area for supersaturation consumption. Note that in case of start-up with ultrasound this sudden change in growth could also be seen, but with a smaller magnitude. In terms of reproducibility between batches, the application of ultrasound performed better compared to unseeded operation and compared to seeds produced with antisolvent crystallization. In terms of

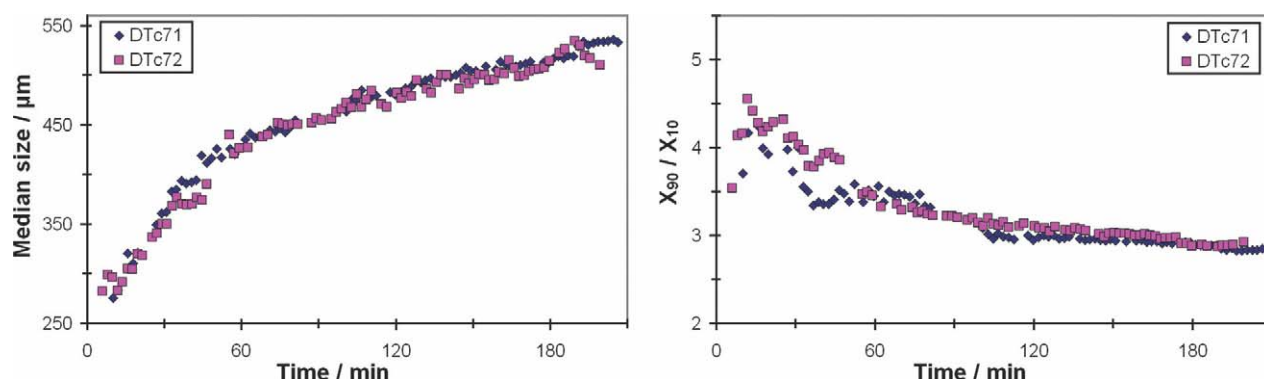


Figure 9. Development CSD as function of time for experiments 75-L DT crystallizer with ultrasound used for start-up expressed in terms of crystal median size (left) and distribution width (right).

The starting point of the batch corresponds with the introduction of the crystals produced with ultrasound. [Color figure can be viewed in the online issue, which is available at www.interscience.wiley.com.]

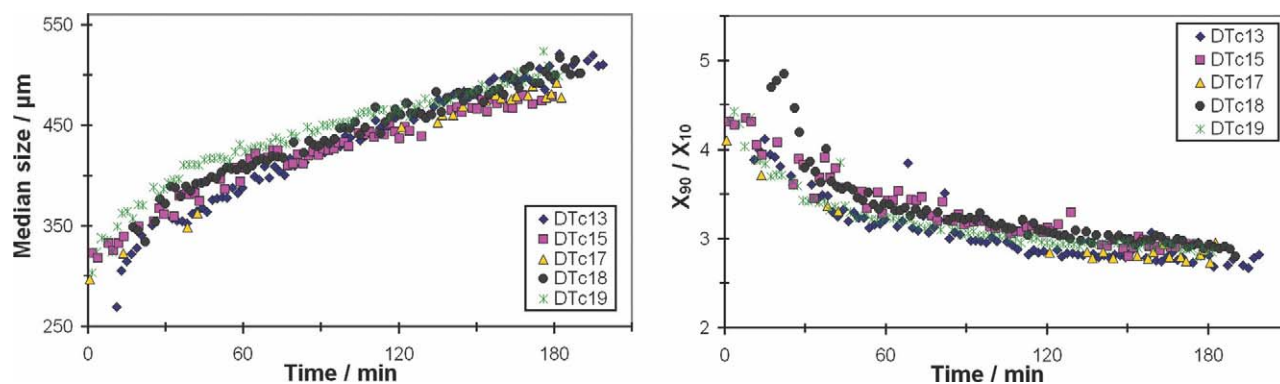


Figure 10. Development CSD as function of time for unseeded experiments 75-L DT crystallizer expressed in terms of crystal median size (left) and distribution width (right), adapted from Ref 1.

The starting point of the batch corresponds with the detection of primary nucleation. [Color figure can be viewed in the online issue, which is available at wileyonlinelibrary.com.]

reproducibility they performed as good as the ground seeds despite the much smaller seed load. In that perspective, the seeds produced with ultrasound proved to be more effective.

The experimental results demonstrate one of the key challenges for applying ultrasound for start-up of batch crystallization on a larger scale. In a relatively small volume, a large amount of nuclei need to be produced. In addition, for in-situ operation the nuclei need to be produced in a small time frame compared to the batch time to provide the same processing experience for each nucleus. For the studied system, an effect of ultrasound could be observed even at low supersaturation, which resulted in a larger amount of produced crystals compared to provoking primary nucleation in a small volume of the crystallizer. Nevertheless, compared to an optimum amount of ground seeds, the amount of produced nuclei was not sufficient to suppress supersaturation in the bulk of the crystallizer provoking significant nucleation throughout the batch, which in the end resulted in a final product with rather broad CSD. Improvements can be expected by exposing the ultrasonic field for a longer time to a supersaturated solution for example by using a flow cell. Alternatively, the ultrasonic field can be intensified in which case a larger amount of the liquid can be insonated effectively.

Conclusions

The effectiveness of the use of an ultrasound probe for start-up of a crystallization process producing ammonium sulfate crystals from aqueous solution in a 75-L DT crystallizer was compared to conventional start-up procedures using unseeded (primary nucleation) or seeded batch strategies. Ultrasound was applied in a small 1.2-L vessel connected to a 75-L DT crystallizer for a quick delivery of the produced crystals into the bulk of the 75-L DT crystallizer.

Quantification of the number of produced crystals with ultrasound revealed the importance of ultrasonic power input, insonation time, and the insonated geometry. A maximum in produced crystals was found for an intermediate power input of 52 W L^{-1} at an initial relative supersaturation of 0.2%, which was well within the metastable zone. The number of produced crystals roughly increased with a factor 10–100 compared to experiments in which ultrasound was not effective. This increase in number of produced crystals was measured for an insonation time of 2 min up to 18 min with the highest value being measured at 6 min of insonation. Depletion of the supersaturation in experiments with a longer insonation time most likely prevented the generation of new nuclei and potentially caused dissolution. In an attempt to maintain constant supersaturation for a longer

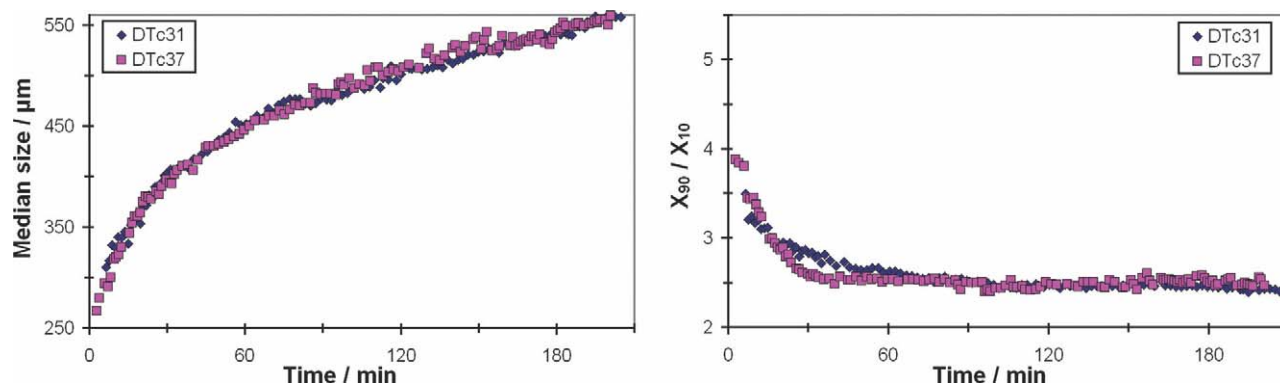


Figure 11. Development CSD as function of time for experiments 75-L DT crystallizer seeded with ground seeds expressed in terms of crystal median size (left) and distribution width (right), adapted from Ref 1.

The starting point of the batch corresponds with the introduction of the seeds. [Color figure can be viewed in the online issue, which is available at wileyonlinelibrary.com.]

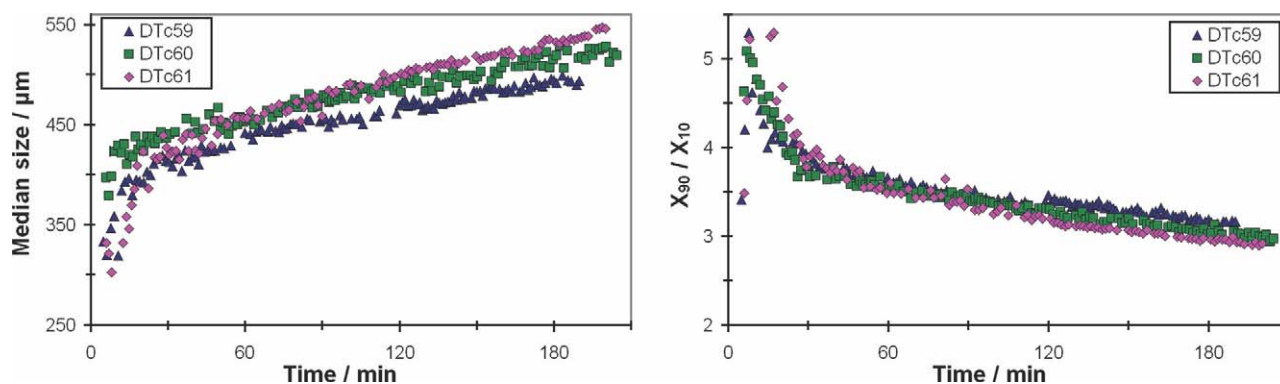


Figure 12. Development CSD as function of time for experiments 75-L DT crystallizer seeded with seeds prepared with antisolvent crystallization expressed in terms of crystal median size (left) and distribution width (right).

The starting point of the batch corresponds with the introduction of the seeds. [Color figure can be viewed in the online issue, which is available at wileyonlinelibrary.com.]

period of time, various cooling ramps were applied from 65°C to 50°C, which were calculated with a model and applied in an open-loop scheme. For those experiments, no trend in number of produced crystals as function of insonation time and cooling profile could be seen and results were comparable to reference experiments in which no ultrasound was applied. The calculated cooling ramp was particularly sensitive for the estimated growth rate, which might have caused significant different supersaturation levels than anticipated resulting in either dissolution of nuclei or conventional primary nucleation.

Various experiments in a vessel with an identical working volume but larger aspect ratio did not show any effect of ultrasound on the number of produced crystals for the tested conditions. A possible cause might be the increased distance ultrasonic waves have to travel to the concave bottom, which reduces mixing. Alternatively, the ultrasonic field might propagate also significantly in radial direction, which is limited for a vessel with a large aspect ratio. The quantification of produced crystals in a smaller volume of a crystallizer demonstrates the importance of a priori screening of operating conditions and the shape of the insonated volume for a given application as only for a limited number of conditions a significant effect of ultrasound was observed on the number of produced crystals for our tested system.

In the next step, the produced crystals with ultrasound in the 1.2-L vessel were used for start-up of experiments in the 75-L DT crystallizer and compared with unseeded experiments and seeded experiments with an optimal amount of ground seeds and seeds produced with antisolvent crystallization in a seeding vessel. The comparison showed that, at least for our application and tested conditions, the use of ground seeds result in better batch performance. The final product quality that was achieved with ground seeds was better, especially in terms of distribution width which was 2.4 (X_{90}/X_{10}) in case of ground seeds and 2.8 in case of start-up with ultrasound. An explanation is that the produced crystals had a smaller seed surface area to consume supersaturation provoking secondary nucleation in the beginning of the batch. The reproducibility between the batches with ultrasound was good, which was also the case for batches in which ground seeds were used for start-up. The reproducibility between unseeded batches or between batches in which seeds produced with antisolvent crystallization were used demonstrated less

reproducibility. The latter method was used to demonstrate typical behavior of a seeded batch with an insufficient surface area, which was caused by agglomeration of the seeds.

The results emphasize the challenges faced when ultrasound is applied on a larger scale for start-up of batch crystallization. A large number of crystals have to be produced in a short amount of time to offer sufficient surface area for supersaturation consumption and to give each nuclei the same processing experience, which results in a narrow product size distribution. The number of produced crystal with ultrasound can be dependent on operating conditions such as supersaturation, insonation time, and power input and on the geometry of the insonated volume. Furthermore, the window in which ultrasound has a clear effect on the number of produced crystals can be rather small. For our tested system, the number of produced crystals was not sufficient to suppress nucleation after introduction in a pilot plant crystallizer, which resulted in a broader final product size distribution compared to an optimum amount of ground seeds. Improvements can be expected by improving the efficiency of ultrasound (power, time, design of the insonated volume, and ultrasound transducers) and increasing the insonated volume for example with flow cells.

Notation

Uppercase letters

B = nucleation rate ($\text{m}^{-3} \text{s}^{-1}$)
 G = growth rate (m s^{-1})
 T = temperature (K)
 V = volume (m^3)
 X = quantile of the CSD

Lowercase letters

k_V = volumetric shape factor
 m_i = i th statistical moment of CSD ($\text{m}^i \text{m}^{-3}$)
 t = time (s)
 w = weight fraction solute (kg kg^{-1})
 w^* = weight fraction solute in saturated solution (kg kg^{-1})
 w_0 = initial weight fraction solute (kg kg^{-1})

Greek letters

σ = relative supersaturation
 ρ_L = density liquid phase (kg m^{-3})
 ρ_S = density solid phase (kg m^{-3})
 ε = volumetric fraction of liquid phase ($\text{m}^3 \text{m}^{-3}$)

Literature Cited

1. Kalbasenka AN, Spierings LCP, Huesman AEM, Kramer HJM. Application of seeding as a process actuator in a model predictive control framework for fed-batch crystallization of ammonium sulphate. *Part Part Syst Charact.* 2007;24:40–48.
2. Richards WT, Loomis AL. The chemical effects of high frequency sound waves. I. A preliminary survey. *J Am Chem Soc.* 1927;49:3089–3100.
3. Li H, Li H, Guo Z, Liu Y. The application of power ultrasound to reaction crystallization. *Ultrason Sonochem.* 2006;13:359–363.
4. Luque de Castro MD, Priego-Capote F. Ultrasound-assisted crystallization (sonocrystallization). *Ultrason Sonochem.* 2007;14:717–724.
5. Lyczko N, Espitalier F, Louisnard O, Schwartzentruber J. Effect of ultrasound on the induction time and the metastable zone widths of potassium sulphate. *Chem Eng J.* 2002;86:233–241.
6. Guo Z, Jones AG, Li N. The effect of ultrasound on the homogeneous nucleation of BaSO₄ during reactive crystallization. *Chem Eng Sci.* 2006;61:1617–1626.
7. Dodds J, Espitalier F, Louisnard O, Grossier R, Hassoun RDM, Baillon F, Gatamel C, Lyczko N. The Effect of ultrasound on crystallisation-precipitation processes: some examples and a new segregation model. *Part Part Syst Charact.* 2007;24:18–28.
8. Guo Z, Zhang M, Li H, Wang J, Kougoulos E. Effect of ultrasound on anti-solvent crystallization process. *J Cryst Growth.* 2005;273:555–563.
9. Kordylla A, Koch S, Tumakaka F, Schembecker G. Towards an optimized crystallization with ultrasound: effect of solvent properties and ultrasonic process parameters. *J Cryst Growth.* 2008;310:4177–4184.
10. Kakinouchi K, Adachi H, Matsumura H, Inoue T, Murakami S, Mori Y, Koga Y, Takano K, Kanaya S. Effect of ultrasonic irradiation on protein crystallization. *J Cryst Growth.* 2006;292:437–440.
11. Kurotani M, Miyasaka E, Ebihara S, Hirasawa I. Effect of ultrasonic irradiation on the behavior of primary nucleation of amino acids in supersaturated solutions. *J Cryst Growth.* 2009;311:2714–2721.
12. Virone C, Kramer HJM, van Rosmalen GM, Stoop AH, Bakker TW. Primary nucleation induced by ultrasonic cavitation. *J Cryst Growth.* 2006;294:9–15.
13. Guo Z, Jones AG, Hao H, Patel B, Li N. Effect of ultrasound on the heterogeneous nucleation of BaSO₄ during reactive crystallization. *J Appl Phys.* 2007;101:054907–054907-9.
14. Amara N, Ratsimba B, Wilhelm A, Delmas H. Crystallization of potash alum: effect of power ultrasound. *Ultrason Sonochem.* 2001;8:265–270.
15. Miyasaka E, Ebihara S, Hirasawa I. Investigation of primary nucleation phenomena of acetylsalicylic acid crystals induced by ultrasonic irradiation—ultrasonic energy needed to activate primary nucleation. *J Cryst Growth.* 2006;295:97–101.
16. Li H, Wang J, Bao Y, Guo Z, Zhang M. Rapid sonocrystallization in the salting-out process. *J Cryst Growth.* 2003;247:192–198.
17. Bund RK, Pandit AB. Sonocrystallization: effect on lactose recovery and crystal habit. *Ultrason Sonochem.* 2007;14:143–152.
18. Kim S, Wei C, Kiang S. Crystallization process development of an active pharmaceutical ingredient and particle engineering via the use of ultrasonics and temperature cycling. *Org Process Res Dev.* 2003;7:997–1001.
19. Higaki K, Ueno S, Koyano T, Sato K. Effects of ultrasonic irradiation on crystallization behavior of tripalmitoylglycerol and cocoa butter. *J Am Oil Chem Soc.* 2001;78:513–518.
20. Ueno S, Ristic RI, Higaki K, Sato K. In situ studies of ultrasound-stimulated fat crystallization using synchrotron radiation. *J Phys Chem B.* 2003;107:4927–4935.
21. Ruecroft G, Hipkiss D, Ly T, Maxted N, Cains PW. Sonocrystallization: the use of ultrasound for improved industrial crystallization. *Org Process Res Dev.* 2005;9:923–932.
22. Ruecroft G. Power ultrasound and particle engineering crystals for drug delivery and formulation. *Chimica Oggi—Chemistry Today.* 2007;25:12–14.
23. Dhumal RS, Biradar SV, Paradkar AR, York P. Ultrasound assisted engineering of lactose crystals. *Pharmaceut Res.* 2008;25:2835–2844.
24. Dhumal RS, Biradar SV, Paradkar AR, York P. Particle engineering using sonocrystallization: salbutamol sulphate for pulmonary delivery. *Int J Pharm.* 2009;368:129–137.
25. Abbas A, Srour M, Tang P, Chiou H, Chan H, Romagnoli JA. Sonocrystallisation of sodium chloride particles for inhalation. *Chem Eng Sci.* 2007;62:2445–2453.
26. Moholkar VS, Sable SP, Pandit AB. Mapping the cavitation intensity in an ultrasonic bath using the acoustic emission. *AIChE J.* 2000;46:684–694.
27. Kordylla A, Krawczyk T, Tumakaka F, Schembecker G. Modeling ultrasound-induced nucleation during cooling crystallization. *Chem Eng Sci.* 2009;64:1635–1642.
28. Daudey PJ. Crystallisation of ammonium sulphate. Ph.D. thesis, Delft University of Technology, 1987.
29. van Iersel MM, Benes NE, Keurentjes JTF. Importance of acoustic shielding in sonochemistry. *Ultrason Sonochem.* 2008;15:294–300.

Manuscript received Jun. 14, 2010, and revision received Dec. 1, 2010.